


RESEARCH ARTICLE

Single-shot phase contrast microscopy using polarisation-resolved differential phase contrast

Ranjan Kalita¹ | William Flanagan¹ | Jonathan Lightley¹ | Sunil Kumar^{1,2} | Yuriy Alexandrov^{1,2} | Edwin Garcia¹ | Mark Hintze³ | Michalis Barkoulas³ | Chris Dunsby^{1,2} | Paul M. W. French^{1,2*} 

¹Photonics Group, Physics Department, Imperial College London, London, UK

²Francis Crick Institute, London, UK

³Department of Life Sciences, Imperial College London, London, UK

*Correspondence

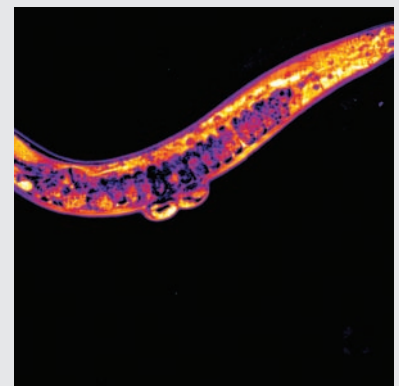
Paul M. W. French, Photonics Group, Physics Department, Imperial College London, London SW7 2AZ, UK.
Email: paul.french@imperial.ac.uk

Funding information

Biotechnology and Biological Sciences Research Council, Grant/Award Number: BB/S506667/1; Cancer Research UK, Grant/Award Numbers: A28450, A29368; Engineering and Physical Sciences Research Council, Grant/Award Number: EP/R511547/1; Medical Research Council, Grant/Award Number: FC001999; Wellcome Trust

Abstract

We present a robust, low-cost single-shot implementation of differential phase microscopy utilising a polarisation-sensitive camera to simultaneously acquire four images from which phase contrast images can be calculated. This polarisation-resolved differential phase contrast (pDPC) microscopy technique can be easily integrated with fluorescence microscopy.



KEYWORDS

phase contrast microscopy, polarisation-resolved imaging, quantitative phase imaging

1 | INTRODUCTION

Phase microscopy is attracting significant interest with the development of quantitative or semi-quantitative techniques that can provide label-free means to image cell dynamics, to aid cell segmentation and or to provide readouts for diverse potential applications [1] such as cell sizing, sorting and/or tracking, microbiology, neuroscience, and pathology. We are particularly interested to explore the potential for label-free segmentation of cells to enhance fluorescence microscopy. There are many approaches to realise quantitative phase microscopy (QPM) including explicit interferometric techniques such as phase stepping interferometry, off-axis (digital)

holography and shearing interferometry, techniques that reconstruct the phase of the electric field scattered by the sample from intensity measurements, such as transport of intensity [2, 3] and (Fourier) ptychography [4], and non-interferometric wavefront sensing approaches including the use of Shack Hartmann sensors [5] or other phase gradient measurement techniques [6, 7], including differential phase contrast microscopy [8, 9]. Most of the phase contrast techniques reported to date require specialist optical components (e.g., objective lenses with phase rings, Nomarski prisms, wavefront sensors), significant modification of the microscope configuration (e.g., for interferometry) and/or the acquisition of multiple images to calculate the phase contrast image. This

This is an open access article under the terms of the Creative Commons Attribution License, which permits use, distribution and reproduction in any medium, provided the original work is properly cited.

© 2021 The Authors. *Journal of Biophotonics* published by Wiley-VCH GmbH.

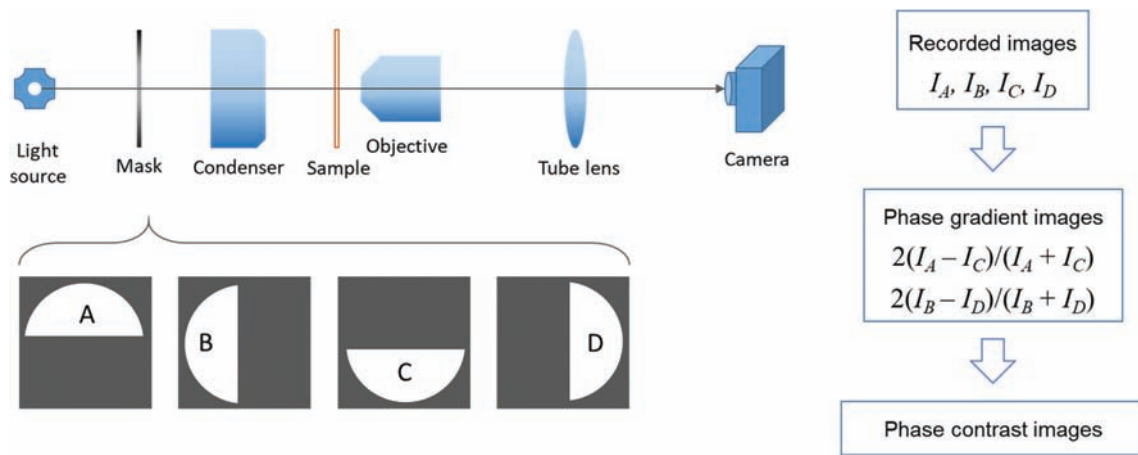


FIGURE 1 Schematic of differential phase microscopy with semi-circular masks in the pupil plane of the condenser lens

can make it challenging to implement these techniques on existing fluorescence microscopes.

Differential phase contrast (DPC) techniques can be conveniently and cost-effectively implemented on existing microscopes by modifying only the illumination path and do not require special objective lenses. The oblique illumination-based DPC approach entails acquiring transmitted light images for different illumination angles, from which semi-quantitative phase images can be reconstructed. An elegant approach to DPC microscopy can be realised by simply acquiring transmitted light images using four illumination directions constrained by semi-circular masks in the back focal plane of the condenser lens, as indicated in Figure 1. This can be conveniently implemented using a liquid crystal device (LCD) in the back focal plane of the condenser lens [10]. Alternatively, this oblique illumination can be provided using a programmable LED array as the illumination source [9]. The phase contrast image may be calculated from a set of four transmitted light images acquired with the condenser pupil plane masks illustrated in Figure 1. The phase gradient images serve as the input data to the convolution calculation outlined in [9], which can be conveniently undertaken using the DPC software [11] shared by the authors of [9] under the GNU General Public Licence version 3.

Usually such oblique illumination DPC techniques require the sequential acquisition of at least two orthogonal pairs of images with semi-circular apertures, each rotated by 180° , in the condenser lens pupil plane. We were motivated to implement a version of oblique illumination DPC microscopy that could acquire quantitative phase images in a single shot, rather than requiring 4 sequential image acquisitions. This would be particularly important to avoid motion artefacts when imaging dynamic samples, for example, live cells or organisms or when cell sorting. A single-

shot implementation DPC microscopy has previously been reported that utilised three colour filters and a colour camera with an RGB Bayer filter sensor [12]. This ‘cDPC’ approach provides single-shot quantitative phase imaging but its use of multiple spectral channels constrains the illumination wavelengths and makes it unsuitable for spectrally resolved imaging. cDPC could be challenged by chromatic aberrations or spectral variations in sample properties and it could be difficult to implement cDPC in a fluorescence microscope without switching the fluorescence filter cube out of the beam path.

We reasoned that if we replaced the conventional camera with a polarisation sensitive camera based on the Sony ‘Polarsens™’ IMX250MZR sensor [13], and distinguished the photons coming from each semicircle in the back focal plane using a polarisation mask, we could acquire 4 images simultaneously at up to 75 frames per second without any spectral trade-offs. As illustrated in Figure S1, the Polarsens™ camera is based on a CMOS sensor integrated with a polarisation filter mask. The 2448×2048 pixels of the CMOS sensor are divided into 1224×1024 ‘super-pixels’. A set of four pixel-sized polarisation filters, with their axis orientated at 0° , 135° , 45° and 90° with respect to the horizontal axis of the sensor, is located in front of each super-pixel (block of 2×2 CMOS pixels labelled 1, 2, 3, 4 in the bottom inset to Figure 2a and Figure S1). Thus, the digital image acquired in a single frame by the Polarsens™ camera can be processed to provide 4 separate polarisation-resolved images (I_1, I_2, I_3, I_4 in Figure 2, which each array all the pixels with the same polarisation filter orientation, that is, I_1 is formed from all pixels with a horizontally orientated filter, etc.). We combine this detector with a polarisation filter mask in the back focal plane of the condenser lens that polarises the illumination light in each of the four quadrants at 0° , 135° , 45° and 90°

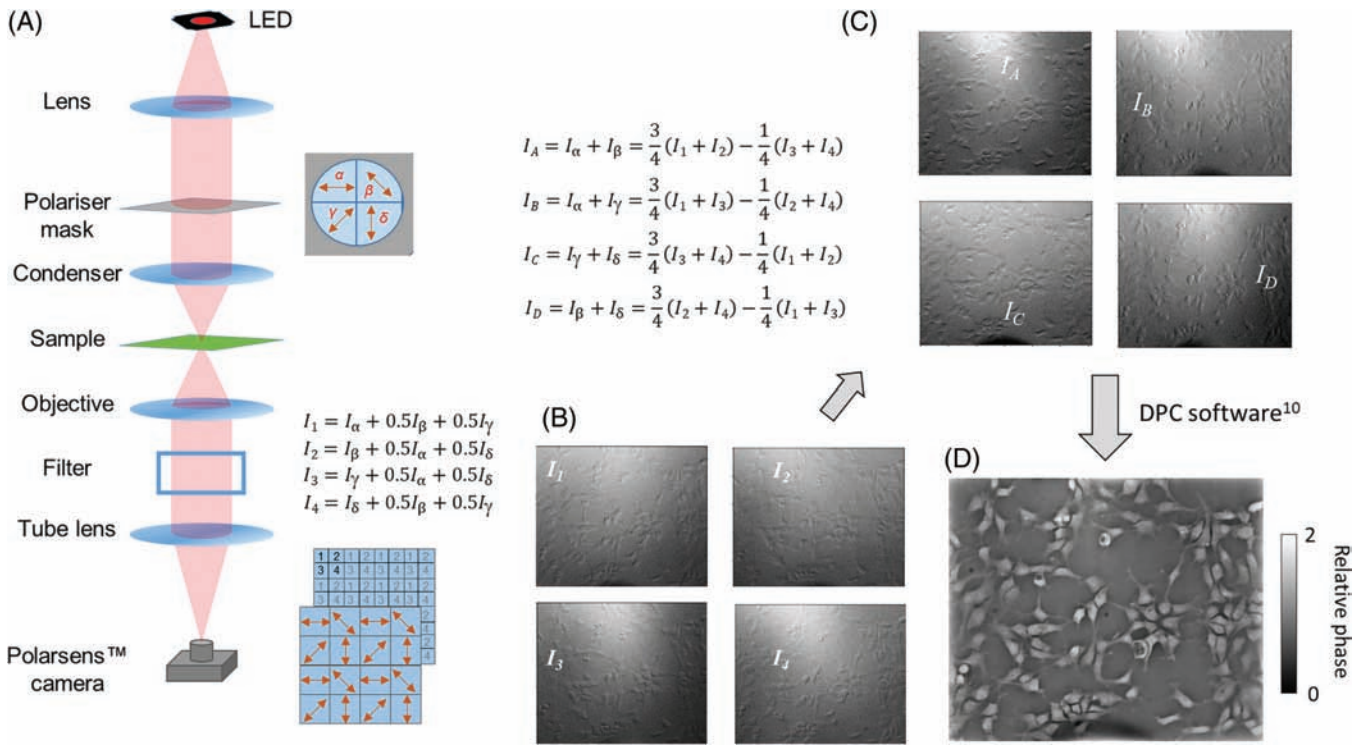


FIGURE 2 Schematic of single shot 'pDPC' microscope utilising a composite polariser in the back focal plane of the condenser lens for which the four quadrants contain polarising film orientated at 0° , 45° , 90° and 135° (the red arrows indicate the axes of polarisation filters). The image acquired on the Polarsens™ camera can be divided into 4 polarisation-resolved images, I_1, I_2, I_3, I_4 . See Figure S1 for an explanation of the operation of the Polarsens™ camera

respectively to realise the technique we describe as polarisation-based differential phase contrast ('pDPC').

Figure 2 presents the principle of pDPC microscopy, which we implemented on a low-cost, modular, open microscopy platform we describe as 'openFrame' [14], using a plug-in developed for Micro-Manager [15, 16] that acquires and processes the polarisation-resolved image data. We aimed to obtain the orthogonal phase gradient images, $2(I_A - I_C)/(I_A + I_C)$ and $2(I_B - I_D)/(I_B + I_D)$, to serve as input data for the DPC software [11] shared by the authors of 9 and to capture these data in a single image acquisition using the Polarsens™ camera (BFS-U3-51S5P-C, FLIR Systems Inc). Accordingly, we fabricated a composite 'quadrant polariser mask' to be located in the condenser pupil plane by mounting 4 pieces of polarising film (Edmund Optics, #86-179) on a glass substrate with the polariser axis for each quadrant (labelled $\alpha, \beta, \gamma, \delta$) orientated at $0^\circ, 45^\circ, 90^\circ$ and 135° . The quadrant polariser mask used for the results presented here was fabricated by cutting the polarising film with scissors to the required quadrant shapes and holding these between a pair of 2-inch diameter glass discs clamped in a threaded aluminium ring, as shown in Figure S2.

For a single image acquisition, the sample is simultaneously illuminated by beams coming from four different directions with four different polarisation orientations (set by the quadrant polariser mask in the back focal plane of the condenser) that are aligned with the four polarisation directions of the pixels on the Polarsens™ camera chip. The four illumination beams contribute intensity distributions $I_\alpha, I_\beta, I_\gamma, I_\delta$, to the image acquired on the camera. As indicated in Figure 2b,c and explained in the Supplementary information, the four polarisation-resolved sub-images (I_1, I_2, I_3, I_4) from the Polarsens™ camera can be used to calculate the set of four images (I_A, I_B, I_C, I_D) corresponding to the images that would be acquired using the condenser pupil plane masks illustrated in Figure 1. This set of images (I_A, I_B, I_C, I_D) can be used to calculate phase gradient images for DPC, that is, $2(I_A - I_C)/(I_A + I_C)$ and $2(I_B - I_D)/(I_B + I_D)$, from which the phase image can be calculated. Here we use the DPC software [11], which is run in MATLAB, as a subroutine called from the pDPC MicroManager plug-in. To calculate the 1224×1024 pixel phase image requires ~1 second on a standard desktop computer. Thus, it is possible to view the phase contrast images in near real time. With improved software, for example, programming in a

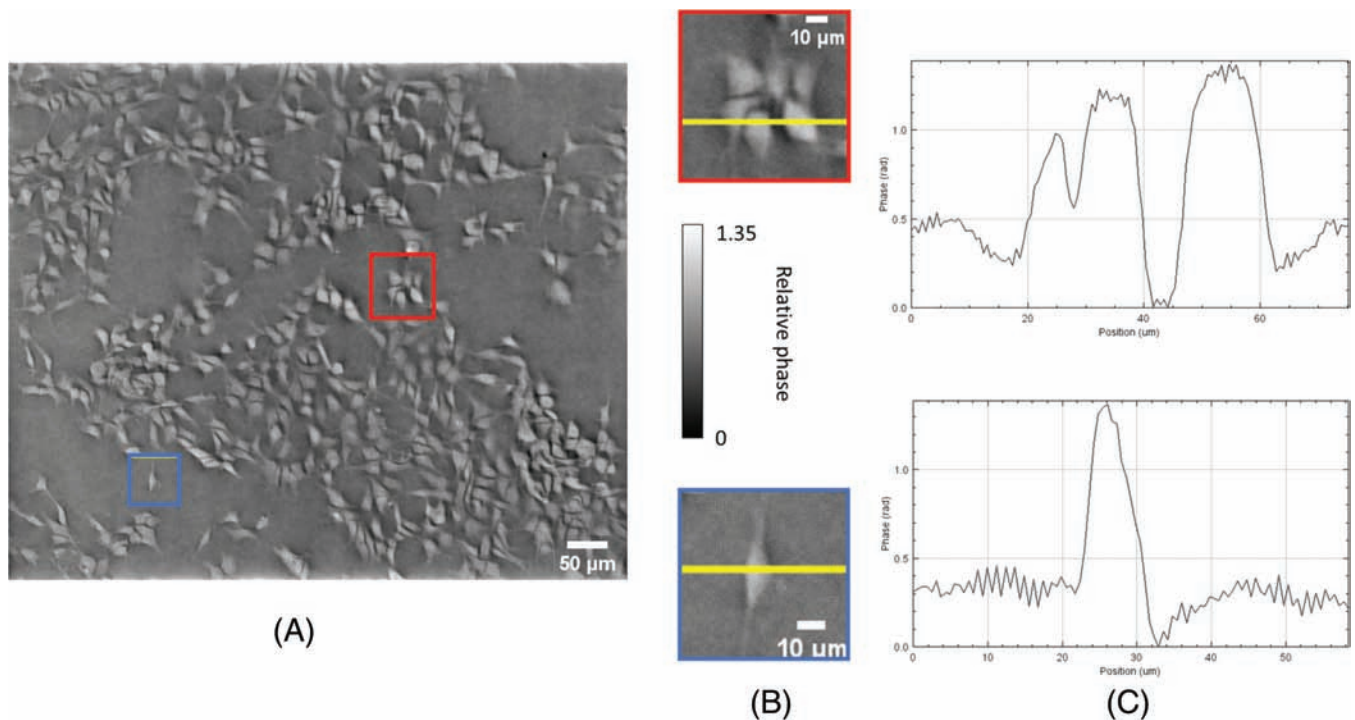


FIGURE 3 A, pDPC phase contrast image of HEK cells images acquired using a $10\times$ 0.3 NA objective lens with 0.36 NA illumination at 560 nm from an LED; B, expanded images of the regions of interest marked in red and blue on, A; C, phase profiles corresponding to yellow lines on, B

lower-level language and/or utilising a GPU, we believe this data processing could be significantly accelerated.

2 | RESULTS

Figure 2 illustrates the application of *pDPC* with exemplar images of HEK cells calculated from a *pDPC* single image acquisition of 30 ms integration time using a 0.4 NA $20\times$ microscope objective lens. The image data was acquired using an *openFrame* fluorescence microscope previously applied to single molecule localisation fluorescence microscopy [17], that was adapted to include a white LED transillumination light source and the transmitted light images were recorded via the fluorescence filter cube to provide a detection channel centred on $590\text{ nm} \pm 55\text{ nm}$. See Figure S5 for a schematic of the microscope configuration. As explained in reference 9, this oblique illumination approach to DPC does not reconstruct low spatial frequency components of the phase contrast image and so the reconstructed phase values are relative to an unknown offset.

Figure 3 shows *pDPC* image data of a similar sample acquired in the same microscope but also using a 10 nm bandpass filter centred at 560 nm; two expanded views of regions of interest are shown with linear phase profiles corresponding to the yellow lines across them. This

illustrates the potential for rapid semi-quantitative phase imaging, which we are exploring to monitor cell dynamics, for high content analysis and for histopathology. Figure S3 illustrates the semi-quantitative nature of *pDPC* compared to standard (qualitative) phase contrast imaging of cells, and Figure S4 shows how *pDPC* phase images of a microlens array can reproduce the spherical profile of the microlenses.

pDPC has no spectral limitation beyond the spectral response of the Polarsens camera ($>400\text{--}700\text{ nm}$) and the properties of the polarisers, in contrast to the *cDPC* approach [12] utilising an RGB sensor, or to the LCD based approach of [10] where the modulation function of a (low-cost) LCD modulator may be limited to a relatively narrow spectral range. Using a suitable illumination source, the broadband nature of our polarisation-based approach to DPC can enable it to be implemented on a fluorescence microscope without changing the fluorescence imaging components; this can facilitate rapid sequential or simultaneous acquisition of fluorescence and phase-contrast images on the same camera without needing to switch the fluorescence filters in the beam path.

Figure 4 shows a raw intensity image and the corresponding *pDPC* phase contrast image of a live *Caenorhabditis elegans* adult acquired using a 0.4 NA $20\times$ microscope objective lens. The *pDPC* image provides superior contrast, clearly resolving anatomical

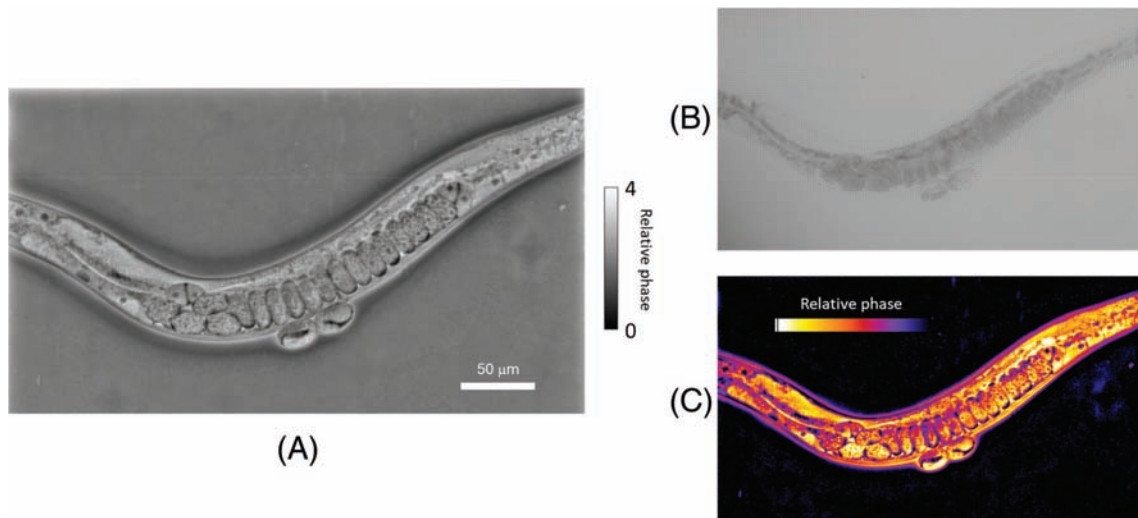


FIGURE 4 A, pDPC image and B, raw transmitted light intensity image of live *Caenorhabditis elegans* adult. C, shows a colour-encoded phase plot of the data presented in, A. This image was acquired with a $20\times$ 0.4 NA objective lens with 0.6 NA illumination

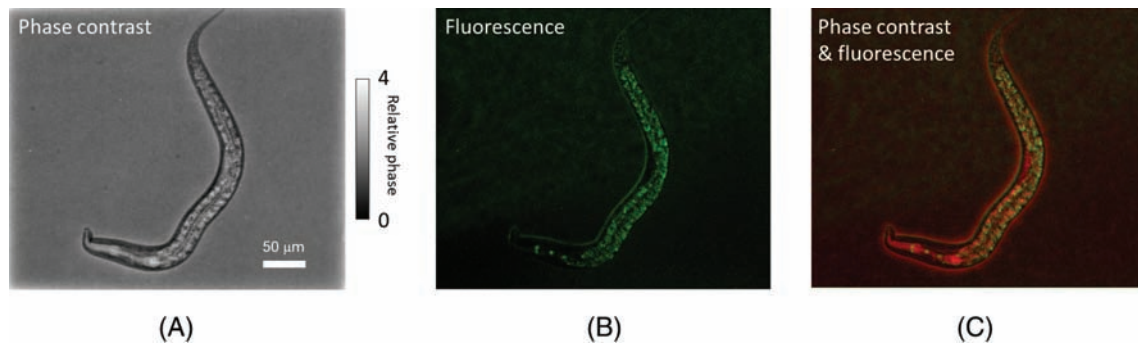


FIGURE 5 A, pDPC phase contrast image; B, GFP fluorescence image and C, overlay of phase contrast (displayed in red) and fluorescence (green) images of live *Caenorhabditis elegans* adult images at $\times 20$ magnification. In panel B, seam cell nuclei can be seen in the head region while intestinal autofluorescence is seen in the rest of the animal body

structures. The capability to study dynamics using pDPC is illustrated in Movie S1, which shows a 2.4 second clip of a live *C. elegans* acquired at a frame rate of 63 frames/s using the same objective lens. The arrow indicates the approximate position of the grinder, which is seen to move during pharyngeal pumping as the animal feeds.

Figure 5 illustrates the capability to acquire co-registered phase contrast and fluorescence images of the same field of view, here applied to a live transgenic *C. elegans* adult in which epidermal stem cell nuclei are labelled with GFP expressed in the lateral seam cells. The same white light LED was used for transillumination and excitation. For the fluorescence image acquisition, an excitation filter (469 ± 35 nm) was placed before the sample and the GFP fluorescence was detected above 520 nm. See Figure S5 for more information concerning the microscope configuration.

3 | CONCLUSIONS

We have demonstrated a single-shot DPC phase contrast technique that utilises a polarisation-resolved camera sensor and can be implemented on most microscopes without requiring any specialised components beyond a custom polarisation mask to be located in the back focal plane of the condenser lens. This mask can be fabricated using low-cost polarising film. The spectral versatility of this pDPC approach enables it to be implemented with multispectral imaging and it can be combined with fluorescence imaging, including to provide co-registered phase contrast and fluorescence images. In principle, the single-shot pDPC image data acquisition can run at the maximum frame rate of the camera (75 full frames/s) enabling phase contrast imaging of dynamic samples including live mobile organisms. As with most phase contrast techniques, including other differential phase

contrast techniques, the performance may vary with the optical properties of different samples and different imaging systems. We note that our pDPC approach reported here does not take into account any polarisation-sensitive properties of the sample that could compromise the calculation of the phase images. However, this is not a problem for most cell-based imaging applications. Future work will include exploiting the Polarsens™ camera to measure sample polarisation properties.


ACKNOWLEDGMENTS

The authors acknowledge helpful discussions with Lei Tian and Laura Waller. Significant components of the instrument reported here were co-designed and fabricated by Simon Johnson, Martin Kehoe and John Murphy in the Optics instrumentation facility of the Physics Department at Imperial College London. We gratefully acknowledge funding from Cancer Research UK (A28450, A29368), and Research England GCRF Institutional Award as well as the Imperial College London Impact Acceleration Accounts supported by the Biotechnology and Biological Sciences Research Council (BBSRC BB/S506667/1) and the Engineering and Physical Sciences Research Council (EPSRC EP/R511547/1). SK and YA are supported by funding from the Francis Crick Institute, which receives its core funding from Cancer Research UK (FC001999), the UK Medical Research Council (FC001999) and the Wellcome Trust (FC001999). Jonathan Lightley acknowledges a PhD studentship from the Engineering and Physical Sciences Research Council. For the purpose of Open Access, the author has applied a CC BY public copyright licence to any Author Accepted Manuscript version arising from this submission.

DATA AVAILABILITY STATEMENT

The data that support the findings of this study are available in Zenodo at <https://doi.org/10.5281/zenodo.4727221>

ORCID

Paul M. W. French  <https://orcid.org/0000-0002-0478-6755>

REFERENCES

- [1] Y. K. Park, C. Depeursinge, G. Popescu, *Nat. Photonics* **2018**, 12, 578.
- [2] M. Shribak, *J. Opt. Soc. Am. A* **2013**, 30, 769.
- [3] C. Zuo, J. Sun, J. Li, J. Zhang, A. Asundi, Q. Chen, *Sci. Rep.* **2017**, 7, 7654.
- [4] G. Zheng, R. Horstmeyer, C. Yang, *Nat. Photonics* **2013**, 7, 739.
- [5] H. Gong, T. E. Agbana, P. Pozzi, O. Soloviev, M. Verhaegen, G. Vdovin, *Opt. Lett.* **2017**, 42, 2122.
- [6] I. Iglesias, *Opt. Lett.* **2011**, 36, 3636.
- [7] A. B. Parthasarathy, K. K. Chu, T. N. Ford, J. Mertz, *Opt. Lett.* **2012**, 37, 4062.
- [8] S. B. Mehta, C. J. R. Sheppard, *Opt. Lett.* **2009**, 34, 1924.
- [9] L. Tian, L. Waller, *Opt. Expr.* **2015**, 23, 11394.
- [10] K. Guo, Z. Bian, S. Dong, P. Nanda, Y. M. Wang, G. Zheng, *Biomed. Opt. Expr.* **2015**, 6, 574.
- [11] <https://github.com/Waller-Lab/DPC>.
- [12] Z. F. Phillips, M. Chen, L. Waller, *PLOS ONE* **2017**, 12, e0171228.
- [13] https://www.sony-semicon.co.jp/products/common/pdf/IMX250_253MZR_MYR_Flyer_en.pdf.
- [14] <https://www.imperial.ac.uk/photronics/research/biophotonics/instruments-software/fluorescence-microscopy/openframe/>.
- [15] A. D. Edelstein, M. A. Tsuchida, N. Amodaj, H. Pinkard, R. D. Vale, N. Stuurman, *J. Biol. Meth.* **2014**, 2014(1), e11.
- [16] <https://micro-manager.org/wiki/>.
- [17] F. Görlitz, J. Lightley, S. Kumar, E. Garcia, M. Yan, R. Wysoczanski, Y. Alexandrov, J. R. Baker, P. J. Barnes, I. Munro, L. E. Donnelly, C. Dunsby, M. A. A. Neil, P. M. W. French, *Proc. SPIE 11076, Advances in Microscopic Imaging II*, 22 July 2019, 1107605. <https://doi.org/10.1117/12.2526940>.

SUPPORTING INFORMATION

Additional supporting information may be found in the online version of the article at the publisher's website.

How to cite this article: R. Kalita, W. Flanagan, J. Lightley, S. Kumar, Y. Alexandrov, E. Garcia, M. Hintze, M. Barkoulas, C. Dunsby, P. M. W. French, *J. Biophotonics* **2021**, 14(12), e202100144. <https://doi.org/10.1002/jbio.202100144>